Salt and Mesophase Formation in Aqueous Suspensions of Lauric Acid

Scott W. Smith[1,2] and Bradley D. Anderson[1,3]

Received March 29, 1993; accepted April 22, 1993

The solubility and solution behavior of lauric acid (LA) and its 1:1 acid soap (potassium hydrogen dilaurate) were investigated at 32°C over a pH range of 2.5–8.5 and at varying KCl concentrations to examine the self-association of this long-chain carboxylic acid under these conditions. LA's solubility in water exhibited the classical pH dependence of a monocarboxylic acid with no evidence of self-association. In 0.1 *M* KCl between pH 6.3 and pH 7.3, filtered samples were turbid, suggesting the presence of high molecular weight aggregates (mesophase), which could be removed by ultrafiltration. The apparent LA solubility vs pH profile in ultrafiltered samples was consistent with a solid phase consisting of either the free acid (pH < 6.5) or potassium hydrogen dilaurate (pH > 6.5), again with no evidence of self-association to form low molecular weight species (dimers, etc.). Quasi-elastic light scattering (QLS) studies and mannitol trapping experiments indicated that vesicles were present in samples containing mesophase. The mesophase composition was characterized and a mass-action law for mesophase formation was developed to describe the apparent LA solubility versus pH in the mesophase region in terms of three parameters. The index of cooperativity, θ, indicated that the mesophase consists of approximately 25 molecules of LA with an acid:anion ratio, ρ, of 1.7. The standard free energy of mesophase formation per mole of monomer was determined to be −6.3 kcal/mol. The aggregate size determined thermodynamically is several orders of magnitude less than that of the mesophase particle size determined by QLS measurements, suggesting that the LA monomer concentration in equilibrium with mesophase may be governed by a small unit domain of the vesicle. These observations may have a bearing on the thermodynamics of self-assembly of lipid bilayer membranes.

KEY WORDS: lauric acid; fatty acids; self-association; mesophase; solubility; lipid bilayers.

INTRODUCTION

Knowledge of the complex physical behavior of fatty acids in water is essential to understand several important biological processes including the transport and metabolism of fatty acids liberated in the intestine during lipolysis, as well as in the circulation and in cells, under conditions that cause the accumulation of fatty acids (1–3) and the enhancement of drug permeability across biomembranes resulting from exposure to medium- and long-chain carboxylic acids (4–6).

Numerous "species" or aggregation states have been previously postulated to rationalize deviations from expected behavior of medium and long-chain carboxylic acids in aqueous solutions. Fatty acids have been theorized to form, in addition to micelles, dimers, or other low molecular weight aggregates (7–15), insoluble acid-soap salts (1,2,16,17), and, more recently, lamellar liquid–crystalline mesophases or vesicles (1,2), depending on temperature, pH, ionic strength, and fatty acid concentration. However, the exact structure, relative stability, and even existence of these aggregates have been debated, and literature values for the thermodynamic parameters governing this complex behavior are generally incomplete or lacking.

The purpose of this study was to examine the solubility and solution behavior of lauric acid (LA) as a function of pH and added KCl at a temperature of 32°C—conditions to be employed in subsequent investigations of the mechanism(s) by which LA enhances solute transport across human skin. Of particular interest were aforementioned reports of the spontaneous formation of lipid bilayer mesophases (1,2) or liposomes (18) under certain conditions from fatty acids varying in chain length from 8 to 18 carbons. Methods developed in this study to monitor LA monomer concentrations in mesophase-containing suspensions enabled us to derive, for the first time to our knowledge, the mass-action law describing formation of a mesophase comprised of lipid bilayers. These studies may have an important bearing on the general problem of the thermodynamics of lipid bilayer self-assembly.

THEORY

Various equilibria, illustrated in Scheme I, have been postulated to account for the solution behavior of fatty acids in aqueous systems. In this section, mathematical relationships are developed to describe the influence of these processes on the solubility of LA versus pH. Experimentally, two apparent solubilities were determined at each pH (see Materials and Methods). LA concentrations in filtered samples were assumed to include the contributions of monomers, low molecular weight aggregates (dimers, etc.) and high molecular weight aggregates (mesophase) to the total apparent solubility, whereas concentrations in ultrafiltered samples (10,000 MW cutoff) were assumed to reflect only the solution concentrations of monomers and low molecular weight aggregates (dimers, etc.).

Predicted pH–Solubility Behavior in the Absence of Self-Association

At 32°C and within the pH range of 2.5–8.5, the solid phase present at equilibrium in aqueous suspensions of LA to which base has been added to adjust pH will be either the free acid or the 1:1 acid-soap (i.e., potassium hydrogen dilaurate when KOH is the base added) (2), depending on the pH. When the solid phase is the free acid, HA, and in the absence of self-association, the solubility behavior of LA will be that of a typical monoprotic weak acid as described by Eq. (1):

$$S = S_o (1 + K_a/\gamma a_{H^+}) \quad (1)$$

where S_o is the intrinsic solubility (i.e., [HA] = S_o), K_a is the ionization constant for LA as depicted in Scheme I, a_{H^+} is

[1] Department of Pharmaceutics and Pharmaceutical Chemistry, University of Utah, Salt Lake City, Utah 84112.
[2] Current address: Glaxo Inc., Five Moore Drive, Research Triangle Park, North Carolina 27709.
[3] To whom correspondence should be addressed.

0724-8741/93/1000-1533$07.00/0

Solid Phase Equilibria

$$HA_{(s)} \overset{S_o}{\rightleftharpoons} HA$$

$$K^+HA^-_{2(s)} \overset{K_{sp}}{\rightleftharpoons} HA + A^- + K^+$$

Ionization Equilibria

$$HA \overset{K_a}{\rightleftharpoons} H^+ + A^-$$

Low Molecular-Weight Aggregates

$$HA + A^- \overset{K_{dh}}{\rightleftharpoons} HA^-_2$$

$$2A^- \overset{K_d}{\rightleftharpoons} [A^-]^{-2}_2$$

High Molecular-Weight Aggregates

$$xHA + yK^+A \overset{K_{meso}}{\rightleftharpoons} \text{Mesophase}$$

$$n\,A^- \overset{CMC}{\rightleftharpoons} \text{Micelle}$$

Scheme I

the hydrogen ion activity, and $\gamma_\pm$ is the mean ion activity coefficient obtained from the modified Debye–Huckel equation (19) [Eq. (2)].

$$\log\gamma_\pm = \frac{-A(I)^{1/2}}{1 + Ba(I)^{1/2}} + bI \qquad (2)$$

where I is the ionic strength of the solution and values of A, B, a, and b at 32°C were obtained from published data (for NaCl solutions) to be 0.518, 0.33, 3.985, and 0.055, respectively (19). Although the ion size parameter, a, has been shown to vary with the ion, solution composition, and solute concentration (20), the solubility data for LA in the presence and absence of 0.1 M KCl and for potassium hydrogen dilaurate at KCl concentrations of 0.03 and 0.1 M were self-consistent when activity coefficients were calculated using Eq. (2).

Equation (1) indicates that the slope of a plot of log$S$ versus pH should asymptotically approach 1 when the pH exceeds the pK_a of LA. However, at sufficiently high concentrations of LA and laurate anion, the 1:1 acid soap, potassium hydrogen dilaurate, is the favored solid phase and the solubility is governed not by Eq. (1) but by the K_{sp} of the 1:1 acid-soap, potassium hydrogen dilaurate, defined [Eq. (3)] in terms of the component activities in solution:

$$K_{sp} = a_{HA}a_{K^+}a_{A^-} \qquad (3)$$

Since $\gamma_{HA} = 1$ at all ionic strengths, $a_{HA} = [HA]$.

The solubility when the solid phase is the 1:1 acid-soap is expressed by Eq. (4):

$$S = \frac{(\gamma_\pm a_{H^+} + K_a)}{\gamma_\pm a_{H^+}} \sqrt{\frac{K_{sp}a_{H^+}}{\gamma_\pm K_a[K^+]}} \qquad (4)$$

One can readily show that, when $[K^+]$ is fixed by the addition of KCl to suspensions, a plot of log$S$ versus pH should have a slope of ½ in the region where the 1:1 acid-soap is the preferred solid phase [i.e., in the pH region 6.5–8.5 (see Results)]. In applying Eq. (4), the solution concentration of LA was assumed to be entirely monomeric and the $[K^+]$ was determined from the charge balance equation:

$$[K^+] = OH^- + f_{A^-}S + Cl^- - H^+ \qquad (5)$$

where Cl^- is the initial KCl concentration and f_{A^-} is the fraction of anion monomer in solution.

Effects of Self-Association

The formation of low molecular weight self-associated species (dimers, etc.) in aqueous solutions of LA would cause positive deviations from the solubility behavior described in Eqs. (1) and (4) as measured by both filtration and ultrafiltration, with the extent of deviation dependent on the magnitude of the association constants. The formation of high molecular weight aggregates would also contribute to positive deviations from Eqs. (1) and (4), but since high molecular weight aggregates would not readily pass through a 10,000 MW-cutoff ultrafiltration membrane, only low molecular weight species would contribute to positive deviations in ultrafiltered samples.

Assuming the primary self-associated species to be either A_2^{-2} or HA_2^- dimers, the apparent solubility in ultrafiltered samples, S_{uf}, may be expressed by Eq. (6):

$$S_{uf} = [HA] + [A^-] + 2K_d[A^-]^2 + 2K_{dh}[HA][A^-] \qquad (6)$$

where K_d is the formation constant for A_2^{-2} dimers and K_{dh} is the formation constant for HA_2^- dimers. Higher-order low molecular weight aggregates could be included by adding additional terms to Eq. (6).

High molecular weight aggregates may exist in the form of micelles formed from fatty acid anions at pH > 9 or liquid crystalline mesophase at lower pH (2) as depicted in Scheme I. Since the pH range of interest in this study was below pH 9, micelle formation was ignored. By analogy with mass-action laws for micelle formation, the mass-action law invoked for mesophase formation assumes that the mesophase is a distinct aggregated species with an equilibrium constant for formation, K_{meso}, defined as

$$K_{meso} = \frac{[\text{Mesophase}]}{[HA]^x(a_{K^+}a_{A^-})^y} \qquad (7)$$

The above relationship further assumes that the mesophase is electroneutral and, as demonstrated experimentally (see Results), contains a fixed ratio of nonionized and ionized fatty acid independent of pH. The molar concentration of mesophase in filtered samples, expressed in terms of the total LA and laurate anion monomer concentration in solution, C_{mon}, is

$$[\text{Mesophase}] = K_{meso}[C_{mon}]^{x+y}(f_{HA})^x(\gamma_\pm^2 f_{A^-}[K^+])^y \qquad (8)$$

where f_{HA} ($= \gamma_\pm a_{H^+}/(\gamma_\pm a_{H^+} + K_a)$) and f_{A^-} ($= K_a/(\gamma_\pm a_{H^+} + K_a)$) are the fractions of free acid and anion monomer, respectively. The parameters K_{meso}, x, and y can be estimated from data for mesophase concentration versus C_{mon}, which can be varied in aqueous suspensions by varying pH.

Initial computer fits of data to Eq. (8) indicated that the parameter pairs x, K_{meso} and y, K_{meso} were highly corre-

lated. Therefore, the following transformations were performed:

$$\theta = x + y \tag{9}$$

$$\rho = x/y \tag{10}$$

$$\epsilon = \frac{\log (K_{meso})}{x + y} \tag{11}$$

where θ is an index of cooperativity reflecting the total number of molecules of free acid and anion combining to form a mesophase unit, ρ represents the free acid:anion ratio in the mesophase, and ϵ is linearly related to the standard free energy per monomer for mesophase formation. The total mesophase concentration using these transformed parameters is expressed by Eq. (12):

$$[\text{Mesophase}] = 10^{\theta\epsilon}[C_{mon}]^{\theta}(f_{HA})^{\rho\theta/(1+\rho)}\{\gamma_{\pm}{}^{2}[K^{+}](1 - f_{HA})\}^{\theta/(1+\rho)} \tag{12}$$

MATERIALS AND METHODS

Materials

Dodecanoic acid (lauric acid, 99–100%; Sigma Chemical Co., St. Louis, MO) and radiolabeled 1-^{3}H-mannitol (30 Ci/mmol; ICN Radiochemicals, Irvine, CA) were utilized without further purification. The 1:1 acid-soap, potassium hydrogen dilaurate ($HA_2{}^{-}K^{+}$), was crystallized from a cold (10°C) methanol solution containing LA and potassium hydroxide (KOH) at molar ratios of 2:1, respectively. The crystals were collected, washed with cold methanol, and dried *in vacuo* at room temperature for 1–2 hr. Potassium laurate was prepared by adding an excess of KOH to an aqueous suspension of LA. The mixture was allowed to stand overnight at room temperature resulting in crystallization of potassium laurate which was collected, washed with water, and dried *in vacuo* overnight. The incongruent melting point (meritectic point) of potassium hydrogen dilaurate was determined by differential scanning calorimetry (DSC) (Model DSC-4, Perkin Elmer, Norwalk, CT) by scanning at 10°C/min over the temperature range of 25–120°C. The purities of the potassium hydrogen dilaurate and potassium laurate were further assessed by titration. A known weight of potassium hydrogen dilaurate was dissolved in warm methanol, titrated initially with 0.1 *N* HCl to determine the amount of $A^{-}K^{+}$, and finally, titrated with 0.1 *N* NaOH to determine the amount of free acid (HA). The acid-anion ratio, $R_{HA:A^-}$, was determined from the relationship

$$R_{HA:A^-} = \frac{V_{ep,\,NaOH} - V_{total,\,HCl}}{V_{ep,\,HCl}} \tag{13}$$

where $V_{ep,\,HCl}$ and $V_{ep,\,NaOH}$ are the volumes of HCl and NaOH titrant required to reach apparent end points in the titrations, and $V_{total,\,HCl}$ is the total volume of acid added as the titrations with HCl were generally taken beyond the equivalence point. Potassium laurate was analyzed by dissolving a known weight of compound in water and titrating with 0.1 *N* HCl.

Solvents used in this study included deionized water, heptane (OmniSolv, EM Science, Cherry Hill, NJ), acetonitrile, and methanol (Baxter Healthcare Corporation, Burdick and Jackson Division, Muskegon, MI). Solutions of HCl, NaOH, and KOH were prepared from DILUT-IT analytical concentrates (J. T. Baker, Inc., Phillipsburg, NJ). All other reagents were analytical grade and obtained commercially.

Titration Analyses

Titrations and pH measurements were performed using a Radiometer (Copenhagen, Denmark) pH meter model PHM82 and a Ross (Boston, MA) combination pH electrode calibrated in commercially obtained buffers.

LA solid phase pH–titration curves were generated in deionized water or in 0.1 *N* KCl by adding a known volume of 0.1 *N* KOH to each of several vials containing suspension (≈50 mg/5 mL water), rotating 15 days at 32°C, and measuring equilibrium pH. Additional base was added to some samples to obtain points at a higher equilibrium pH (>8.0). These samples were equilibrated an additional 3 days.

Titrations were also performed to determine mesophase composition. Samples in plastic vials ranging from pH 6.3 to 7.0 were prepared by adding HCl or KOH to suspensions of potassium hydrogen dilaurate or LA or both in 0.1 *M* KCl and equilibrating at 32°C. These samples were turbid, indicating the presence of mesophase. Aliquots (0.5 mL) were filtered (0.45 μm), diluted with 0.1 *M* KCl (2 mL) and heptane (0.5 mL), and titrated with 0.1 *N* HCl to determine total anion concentration. The contribution of anion in the mesophase, $[A^-]_{meso}$, to the total molar concentration of anion was obtained by Eq. (14):

$$[A^-]_{meso} = N_{HCl}V_{ep}/V_T - C_{uf}K_a/(\gamma_{\pm}a_{H^+} + K_a) \tag{14}$$

where V_{ep} is the volume of 0.1 *N* HCl required to reach an apparent end point, V_T is the total solution volume, and C_{uf} is the total LA concentration in the ultrafiltrate. The contribution of free acid in the mesophase, $[HA]_{meso}$, was then obtained by the difference

$$[HA]_{meso} = C_f - C_{uf} - [A^-]_{meso} \tag{15}$$

where C_f is the total LA concentration in filtered samples. The mesophase titrations were validated in separate titrations of known concentrations of potassium laurate varying in concentration and in the presence of added free LA.

Analysis of Lauric Acid by Capillary Gas Chromatography

LA concentrations were determined by capillary gas chromatography (GC) (Model 5890A, Hewlett-Packard, Palo Alto, CA). Filtered or ultrafiltered aqueous solutions (0.5 mL) were acidified with phosphoric acid to pH < 3, and heptane (0.5 mL) was added to extract LA from the aqueous phase. After vortexing the two-phase mixture, the heptane layer was removed with a pipette and transferred to a sample vial. Heptane samples (1–5 μL) were injected (Model 7673A auto injector, Hewlett-Packard, Palo Alto, CA) onto a methyl silicone HP-1 column (10 m × 530 μm × 2.65-μm film thickness) at an oven temperature of 155°C. The injector port and flame ionization detector temperatures were maintained at 250°C. Helium was used as a carrier gas at a flow rate of 15 mL/min with split ratios (split vent:column flow rates) of 20:1 to 1:1 depending on the sample concentration. The re-

tention time for LA was 2.5–2.7 min. Peak areas were recorded with an integrator (Model 3396 A, Hewlett-Packard, Palo Alto, CA). Solution concentrations analyzed ranged from 10^{-4} to 10^{-2} *M*. The heptane extraction efficiency was determined to be 99.2%. Adsorption of LA within the injector port was minimized by replacing a stainless-steel insert seal with a gold-plated one and frequent replacement of inserts and the silanized glass wool. Detector response was linear over a concentration range that spanned one order of magnitude encompassing the analyte concentrations with coefficients of variation in response factors (ratio of standard concentration to peak area) of <5%.

Solubility Determinations

Solubilities were determined by adding an excess of LA crystals to glass or plastic vials containing 10 mL of either deionized water or 0.1 *M* KCl. Initial pH was adjusted with HCl or KOH from 2.5 to 8.5. Additional solubility determinations to confirm the K_{sp} of potassium hydrogen dilaurate were conducted by using an excess of the 1:1 acid-soap in glass or plastic vials containing 10 mL of 0.03 or 0.1 *M* KCl. Initial pH was adjusted to 6.2–8.5 with HCl or KOH. Vials were sealed under nitrogen to exclude CO_2 and shaken in a water bath at 32 ± 0.5°C until pH and filtrate concentrations were constant for at least 48 hr. This generally required 5–10 days in samples containing only LA solid and no mesophase and 15–20 days in samples containing mesophase. When mesophase was present in the suspension, further adjustment of pH during the experiment was usually necessary to obtain data spanning the desired region. At equilibrium the pH was recorded and aliquots were filtered with a 0.45-μm syringe filter (Acrodisc-3, Gelman, Ann Arbor, MI) to remove crystalline particles and/or ultrafiltered to remove both solid particles and high molecular weight aggregates.

Ultrafiltration of samples was conducted by placing an aliquot (0.5 mL) in the sample reservoir of a microconcentrator cartridge (Amicon Centricon-10, Danvers, MA) that had previously been stored at 32°C. The cartridge was immediately centrifuged (Sorvall RC2B, Newtown, CT) at 5000 rpm for 10–40 min at 32°C (temperature range was 28.5–34°C) which forced the sample to pass through a 10,000 MW-cutoff filter. The ultrafiltrate was collected in a cup attached to the cartridge. Several aqueous solutions of LA were prepared ranging in concentration from 10^{-5} to 10^{-3} *M*, and the concentrations were measured before and after ultrafiltration to assess the extent of LA retention by the ultrafiltration membrane. For each solution, successive aliquots of 0.5 mL were collected from a single ultrafilter and analyzed. To validate the ultrafiltration method further, a 1.0-mL sample from a turbid suspension of potassium hydrogen dilaurate at pH 6.5 in 0.1 *M* KCl was ultrafiltered, and several fractions (90–100 μL) were collected. The LA concentration was determined for each fraction in order to assess whether or not the concentration was affected by removal of fluid from the sample reservoir during ultrafiltration.

LA concentrations in filtered or ultrafiltered samples were determined by capillary GC (*vide supra*). A least-squares optimization program, MINSQ (MicroMath, Salt Lake City, UT), was used to analyze the solubility data in order to obtain various thermodynamic parameters.

Mesophase Particle Size Determination

The average hydrodynamic radius, R_h, and index of polydispersity, *V*, for mesophase particles were determined by quasi-elastic light scattering (QLS). The equipment employed in QLS measurements included a Cooper Laser Sonics (Palo Alto, CA) argon ion laser (Model 95) at a wavelength of 514.5 nm, a temperature-controlled scattering cell holder maintained at 32°C, a Brookhaven (Holtsville, NY) goniometer, and a Brookhaven autocorrelator (Model BI-2030AT). Aliquots (1.0 mL) were filtered (0.45-μm pore size) into a clean (washed with chromic acid solution) glass test tube that was preheated to 32°C. These test tubes were sealed and immediately placed in the cell holder. Scattered light was collected 90° to the incident light. R_h and *V* values were determined by a cumulant analysis of the intensity autocorrelation function fit to a cubic equation.

Dispersions analyzed included samples which had been equilibrated for 10–15 days at 32 ± 0.5°C in KCl concentrations ranging from 0.0 to 0.3 *M*. An additional set of samples was prepared by preheating suspensions to 50°C for 2 hr prior to equilibration at 32°C for 10–15 days to determine if the route of preparation affected the final equilibrium particle size. Finally, a sample in 0.1 *M* KCl, previously equilibrated at 32°C, was sonicated for 10 min and shaken in a water bath (both at 32°C). The R_h of this sample was monitored over a 10-day period following sonication.

The effect of mesophase turbidity on the precision of QLS measurements was determined. Serial dilutions of polystyrene bead suspensions (Duke Scientific, Palo Alto, CA) with a reported diameter of 87 ± 4 nm were prepared. The turbidity of mesophase and polystyrene bead suspensions was quantified by measuring the absorbance at 400 nm. Only when the absorbance was greater than 0.8 AU for the polystyrene bead suspensions were the experimentally determined particle sizes by QLS smaller than the reported size range (i.e., diameter less than 83 nm). Since the maximum absorbance for the mesophase samples was 0.6 AU, the error in the particle size of mesophase samples due to sample turbidity was assumed to be negligible.

Mannitol Trapping by Lauric Acid Mesophase

Suspensions containing excess potassium hydrogen dilaurate and LA were equilibrated in 0.1 *M* KCl at 32°C in the presence or absence of 1-^{3}H-mannitol (0.04 μCi/mL). Filtrates of these suspensions were turbid, suggesting the presence of mesophase. Control samples prepared in an identical fashion but without mannitol were spiked with 1-^{3}H-mannitol to obtain a final concentration of 0.04 μCi/mL immediately (within 60 sec) prior to size-exclusion chromatography.

Size exclusion chromatography was employed to separate free mannitol from entrapped mannitol. A column (PD-10, Pharmacia, Uppsala, Sweden) packed with Sephadex G-25M (bed volume, 9.0 mL; void volume, 2.5 mL) was utilized. The column and mobile phase (0.1 *M* KCl adjusted to pH 6.5) were maintained at 32°C. The mobile phase also contained 6.0×10^{-4} *M* LA, equal to the monomer concentration in mesophase samples, in order to minimize dissociation of mesophase during the chromatography. The column was saturated with 50 mL of eluant prior to the introduction

of a 250-μL aliquot of filtered sample containing mesophase. Twelve 1.0-mL fractions were collected and the amounts of mannitol were determined on a scintillation counter (LS 1801, Beckman Instruments Inc., Fullerton, CA) after diluting a 50-μL aliquot of sample with 2.0 mL of Opti-Fluor cocktail (Packard Inst. Co., Inc., Meriden, CT). LA concentrations in each fraction were determined by capillary GC as described previously.

RESULTS

Potassium Laurate and Potassium Hydrogen Dilaurate Purity Determinations

The molar ratio of free acid to laurate anion, $R_{HA:A^-}$, was determined for three independently prepared batches of potassium hydrogen dilaurate by titration with HCl and KOH to be 0.96 ± 0.05. From the titration data the equivalent weight of potassium hydrogen dilaurate, which has a theoretical value of 219.3, was determined to be 219.2 ± 0.2. Likewise, an equivalent weight for potassium laurate was determined by titration to be 238.8 (theory, 238.3).

An endotherm corresponding to the meritectic point of potassium hydrogen dilaurate was observed by DSC with an onset temperature of 94.9°C and a peak width of 92 to 103°C at a scan rate of 10°C/min, consistent with a reported meritectic point of 94°C (21). An endotherm with an onset temperature of 55.1°C was observed for potassium laurate in agreement with the reported phase transition temperature of 57°C (21).

Solid Phase Behavior of Lauric Acid Versus Solution pH

Shown in Fig. 1 are plots of equilibrium pH versus amount of KOH added to suspensions of LA in deionized water or 0.1 *M* KCl. The pH initially increased and then reached a plateau with increasing KOH added. The plateau pH value was dependent on [KCl] (i.e., pH 7.6 when no KCl was added; pH 6.5 in 0.1 *M* KCl). Cistola *et al.* (2) have shown that the solid phase in this plateau region contains both LA crystals and 1:1 acid-soap crystals (potassium hydrogen dilaurate). Beyond the plateau regions in Fig. 1, the pH again increased with the addition of base, and the solid phase was shown by titration to be pure potassium hydrogen dilaurate. Therefore, the plateau regions in Fig. 1 reflected a transition in the solid phase from LA to potassium hydrogen dilaurate. These results indicate that discontinuities are to be expected in the pH–solubility profiles at a pH of 7.6 in the absence of added KCl and at pH 6.5 in 0.1 *M* KCl due to changes in the solid phase composition.

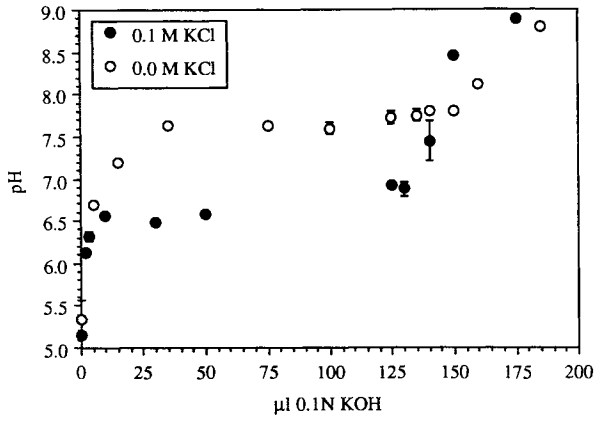

Fig. 1. Titration of aqueous suspensions initially containing crystalline lauric acid in either deionized water or 0.1 *M* KCl with 0.1 *N* KOH at 32°C. At pH values below the plateau region, the solid phase was lauric acid, and above the plateau region, potassium hydrogen dilaurate was the solid phase. The plateau region reflects a change in the solid phase from lauric acid to potassium hydrogen dilaurate as base is added. The difference in plateau pH with KCl concentration indicates that at least one degree of freedom is present in the system.

Lauric Acid Solubility–pH Behavior

A semilog plot of the aqueous solubility of LA versus pH in deionized water is shown in Fig. 2. Solubilities were determined only in the region where the solid phase was LA. The curve approached a slope of unity as pH increased, characteristic of a monoprotic weak acid in the absence of self-association, as expressed by Eq. (1). The intrinsic solubility, S_o, and pK_a of LA were determined to be 1.34 (±0.14) × 10^{-5} *M* and 4.94 ± 0.06, respectively, by nonlinear regression analysis. The fitted line is shown in Fig. 2. The values for these parameters are similar to published data (22).

Solubility data were also obtained for LA in 0.1 *M* KCl over the pH range 2.5–8.5, which includes the region where both solids (LA and potassium hydrogen dilaurate) may exist. Apparent solubilities obtained from filtered samples are shown in Fig. 3. Beginning at approximately pH 6.3, the filtrate concentrations deviated from the solubility curve predicted by Eq. (1). The filtrate concentrations rapidly increased, reached a maximum at pH 6.5, and decreased with pH until, near pH 7.3, the slope of the line for the logarithm of the filtrate concentration became linear with a value of 0.5.

The unexpected peak in apparent solubility was accompanied by marked turbidity in filtered samples suggesting the presence of high molecular weight aggregates. Turbidity was absent below pH 6.3 or above pH 7.3. Turbidity was also observed in samples from the plateau regions in Fig. 1.

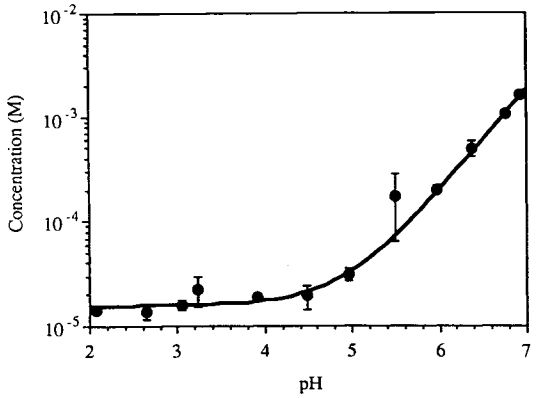

Fig. 2. Solubility–pH profile of lauric acid at 32°C in deionized water. Regression analysis of data, shown by the solid line, provided values for intrinsic solubility and ionization constant which are listed in the text.

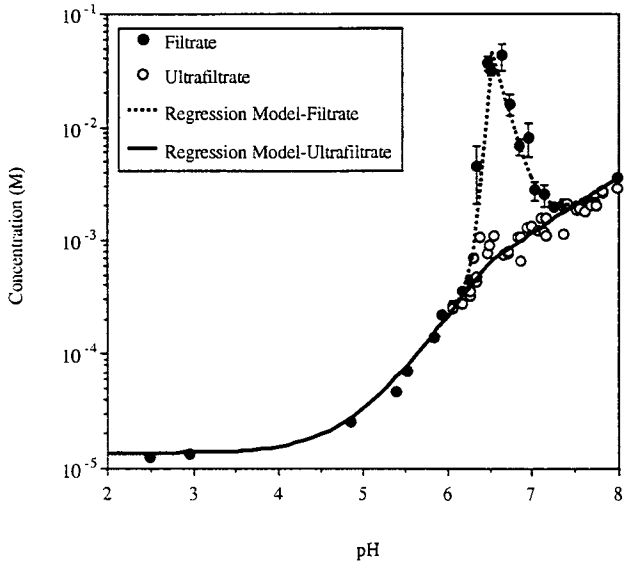

Fig. 3. Concentrations of lauric acid versus pH in filtered or ultrafiltered samples of lauric acid (pH <6.5) or potassium hydrogen dilaurate (pH >6.5) suspensions in 0.1 *M* KCl at 32°C. The solid line assumes that the solubility, as determined in ultrafiltered samples, is governed by Eq. (1) below pH 6.5 and by Eq. (4) above pH 6.5. The dashed line represents the regression analysis of the filtered sample data and therefore includes the mesophase concentration described by Eq. (12).

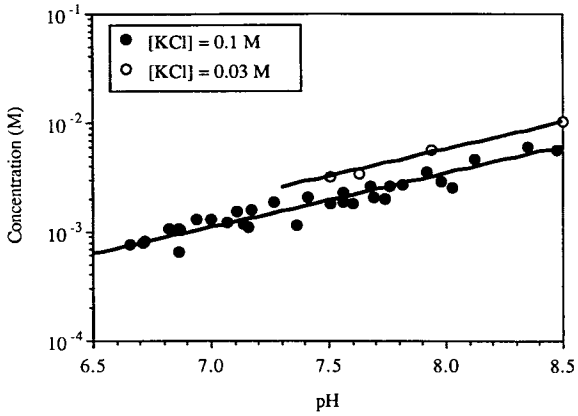

Fig. 4. Lauric acid concentration versus pH in ultrafiltered samples of potassium hydrogen dilaurate suspensions in 0.03 or 0.1 *M* KCl at 32°C. The solid lines reflect the K_{sp} for potassium hydrogen dilaurate determined by nonlinear regression analysis according to Eq. (4).

Optically clear samples were obtained by ultrafiltering turbid solutions through a 10,000 MW-cutoff filter which effectively removed large aggregates but should have allowed smaller self-associated species to pass. The concentrations of LA in solutions varying in pH were measured before and after ultrafiltration in order to measure sample recoveries. Using the Centricon-10 ultrafiltration device, the concentrations in ultrafiltrates were constant after the first 0.5–1.0 mL and yielded an average recovery of 95 ± 2% (mean ± SE) over the pH ranges and concentrations explored. No trend was apparent in ultrafiltrate concentration with the volume of sample ultrafiltered.

Concentrations of LA from ultrafiltered samples are also shown in Fig. 3. At pH 6.5 a distinct discontinuity occurred in this profile, with the slope changing from ≈1.0 to 0.5, consistent with a change in composition of the solid phase from LA (pH < 6.5) to potassium hydrogen dilaurate (pH > 6.5). The solubility behavior of LA in the presence of potassium hydrogen dilaurate should be governed by its solubility product, K_{sp}, defined in Eq. (3). To define the K_{sp} more carefully, additional solubility data were obtained in suspensions of potassium hydrogen dilaurate prepared in 0.03 *M* KCl. Figure 4 shows the LA ultrafiltrate concentrations in 0.03 *M* KCl over the pH range of 7.5–8.5 and in 0.1 *M* KCl over the pH range 6.5 to 8.5. These data were analyzed by nonlinear regression to obtain K_{sp} by using Eq. (4). The lines in Fig. 4 represent the fit of Eq. (4) to the data (coefficient of determination = 0.99). The value obtained for K_{sp}, 5.25 (±0.13) × 10^{-10}, is similar to the value previously reported at 20°C by Lucassen (17). (Lucassen defined the K_{sp}' of potassium hydrogen dilaurate as the product $a_{K^+}a_{H^+}a_{A^-}{}^2$. Using a K_{sp}' of 6.31 × 10^{-15} and a K_a of 1.25 × 10^{-5} reported by Lucassen at 20°C, a value of 5.04 × 10^{-10} is obtained for K_{sp} as defined in this paper.)

From the values for S_o, K_a, and K_{sp} determined above, it is possible to describe the apparent solubility of LA obtained by ultrafiltration over the entire pH and [KCl] range examined without the necessity to invoke self-association of LA to form low molecular weight aggregates. The calculated (solid) line through the ultrafiltrate data in Fig. 3 reflects these parameters.

The LA concentrations in filtered samples were superimposable on the concentrations in ultrafiltered samples below pH 6.3 and above pH 7.2, suggesting that, in these regions, only solid LA or potassium hydrogen dilaurate exist in equilibrium with monomer in solution. However, Fig. 3 clearly highlights the turbid region where high molecular weight aggregates appear to predominate.

Mesophase Characterization

Turbid samples were examined by QLS to determine the average hydrodynamic radii, R_h, and index of polydispersity of the mesophase particles. R_h values ranged from 90 to 175 nm, with no apparent trend between particle size and KCl concentration. The index of polydispersity ranged from 40 to 60%. Typically observed indices of polydispersity in monodisperse systems are 10 to 20% (23), indicating that the mesophase consisted of a heterogeneous mixture of particles. However, since an index of polydispersity greater than 60% is necessary in order for light-scattering measurements to distinguish between two different populations of particles (23), the question of whether or not the mesophase consisted of two or more distinguishable types of particles (e.g., vesicles and smaller fragments) could not be addressed by this technique.

Samples which had been preheated for 2 hr at 50°C prior to equilibration at 32°C exhibited no significant changes in either average particle size or polydispersity in comparison with samples which had not been preheated, suggesting that the mesophase was at an equilibrium particle size. Sonication of a sample in 0.1 *M* KCl equilibrated at 32°C resulted in an initial increase in size from ≈90 to ≈200 nm within the

first 2 hr after sonication and a change in polydispersity from 50% before sonication to 15% 2 hr after sonication. After 10 days at 32°C, however, the particle size and index of polydispersity returned to their original (before sonication) values, within experimental error.

The composition of mesophase was determined by titrating samples in the mesophase region with 0.1 *N* HCl to determine total laurate anion concentration, which, after correcting for the anion monomer in ultrafiltrate gave the anion concentration in the mesophase. The ratio of anion concentration to total LA concentration in the mesophase, determined by capillary GC, gave the molar fraction of anion in the mesophase. This fraction was constant with pH, averaging 0.32 ± 0.04 (n = 7) over the pH range 6.5 to 6.94 with no trend apparent.

The sensitivity of mesophase concentration and composition to KCl concentration was also determined. Figure 5 shows the LA concentrations in filtrate and calculated monomer concentrations in suspensions containing excess LA and potassium hydrogen dilaurate at varying KCl concentration. The formation of mesophase is highly dependent on KCl concentration, and at sufficiently high [KCl] (e.g., 0.3 *M*), mesophase could no longer be detected. The molar fraction of anion in these mesophases averaged 0.39 ± 0.06 but large standard deviations were evident in the data at 0 and 0.2 *M* KCl due to the small differences between the filtrate and the ultrafiltrate concentrations at these extremes. Therefore, the titrations suggest that mesophase composition does not vary significantly with KCl concentration in the range of 0.05–0.1 *M* KCl but provide less information on the composition outside of this range.

The existence of vesicles in the mesophase region was investigated by ^{3}H-mannitol trapping experiments. Samples containing mesophase (equilibrium LA filtrate concentration was 0.07 *M*) equilibrated at 32°C in the presence of 1-^{3}H-mannitol were filtered through a size exclusion column to separate trapped from free mannitol. Figure 6A shows the LA concentration and amount of mannitol present in collected eluant fractions. The maximum LA concentration was observed at an eluant volume corresponding to that of the column void volume, consistent with the elution of large

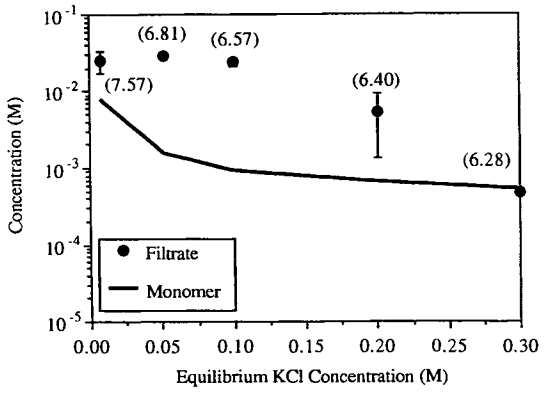

Fig. 5. Lauric acid concentration in filtrates from suspensions of lauric acid and potassium hydrogen dilaurate varying in KCl concentration compared to the theoretical monomer concentrations at 32°C. pH values measured at equilibrium are shown in parentheses adjacent to each point.

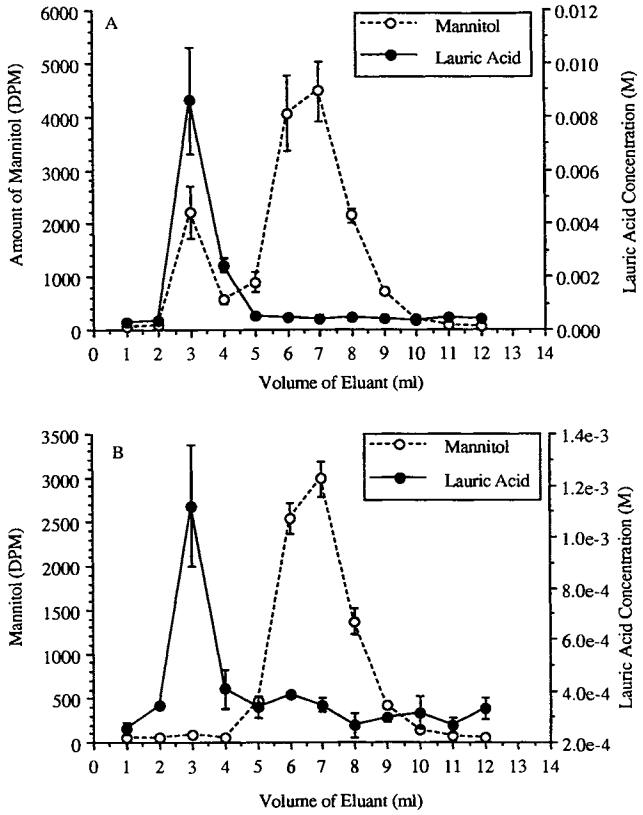

Fig. 6. Lauric acid and ^{3}H-mannitol concentrations in eluant fractions collected from size-exclusion chromatographic analysis of a mesophase sample equilibrated with mannitol at 32°C (A) or spiked with mannitol and immediately chromatographed at 32°C (B).

mesophase particles. A mannitol peak eluted at the same time as the mesophase, while the remaining free mannitol eluted at 6–7 mL. The percentage of total volume trapped by the mesophase, calculated from the relative areas of trapped and free mannitol, was ≈13%. The results of a control experiment in which mannitol was added to a sample containing mesophase followed immediately by size exclusion chromatography are shown in Fig. 6B. There was no evidence of entrapped mannitol under these conditions.

A theoretical trapped volume was estimated by assuming that the mesophase consisted of unilamellar vesicles with a radius of 1000 Å, a surface area per head group of 35 Å (1), and a bilayer thickness of 30 Å (24). From these dimensions, vesicle size and number of monomers per vesicle were calculated. The total number of vesicles, and hence the total enclosed volume, was calculated from the total LA concentration of 0.07 *M*. A theoretical enclosed volume of 23% was calculated, in reasonable agreement with the experimental value of 13%. The possible presence of multilamellar vesicles or polydispersity of these systems may account for the slightly lower than predicted experimental trapped volumes.

Mass-Action Law for Mesophase Formation

Knowledge of both monomer and mesophase concentrations provided the opportunity to investigate the mass-action law for mesophase formation. The concentrations of LA in mesophase, obtained from the data in Fig. 3, were

examined by nonlinear regression analysis according to Eq. (12), where C_{mon} was calculated from Eq. (1) when the solid phase was LA or Eq. (4) when the solid phase was potassium hydrogen dilaurate. Values for the three parameters, θ, ρ, and ϵ, obtained from regression analysis of the mesophase region (dashed line in Fig. 3) are listed in Table I.

DISCUSSION

Solid Phase Behavior of Lauric Acid Versus Suspension pH

The results in Fig. 1 confirm previous reports that the solid phase present in suspensions of LA depends on solution pH and KCl concentration (16–18). Figure 1 illustrates that it is necessary to specify the potassium chloride concentration in order to uniquely define the composition (i.e., pH) of the aqueous phase when both solid LA and potassium hydrogen dilaurate are present. Cistola *et al.* (2) and Feinstein (16) independently described regions in the titration of micellar solutions with HCl where the pH appeared to be invariant with the addition of titrant. This plateau region reflected the transition from potassium hydrogen dilaurate to crystalline lauric acid with the addition of HCl. Cistola *et al.* argued that under these conditions, the system contained three components (potassium laurate, water, and HCl) and three phases (crystalline lauric acid, potassium hydrogen dilaurate, and the aqueous solution); therefore, according to the Gibbs phase rule, $F = C - P$ at constant temperature and pressure, the system was uniquely defined (i.e., zero degrees of freedom). Hence, the pH, or the composition of the system, could not change as acid was added to the system.

For a system in thermodynamic equilibrium, the chemical species that are considered components, C, in the Gibbs phase rule must completely describe the composition of each phase (25). A practical method for determining the number of components is to set it equal to the number of independent chemical constituents in the system minus the number of distinct chemical reactions that can occur between these species. In the titration of potassium laurate with HCl there are six constituents when both solids are present (K^+A^-, HA, $HA_2^-K^+$, H_2O, KCl, and HCl) and two chemical reactions between these constituents ($HCl + K^+A^- \rightleftharpoons KCl + HA$ and $HA_2^-K^+ \rightleftharpoons HA + K^+A^-$). Therefore, there are four components and one degree of freedom (at constant temperature and pressure) in the plateau region shown.

Previous experiments have demonstrated (16,18) that when both solid phases were present, the pH decreased as HCl was added to the system, consistent with the predictions of the Gibbs phase rule. Although pH did not appear to change in the plateau regions described by Cistola *et al.* (2), a decrease of only 0.24 pH unit would be expected according to theory and, therefore, may not have been detected. In contrast to the results obtained by titration with acid, addition of KOH to a suspension of lauric acid would not alter the solution composition when both solids are present, as KOH would be consumed in the conversion of lauric acid to potassium hydrogen dilaurate. Therefore, pH was constant in the plateau regions of Fig. 1.

The presence of a mesophase (an additional constituent) in the plateau regions of Fig. 1 would not change the above interpretation, since an additional chemical reaction can be invoked between this constituent (considered as a species in solution rather than a separate phase) and lauric acid and potassium laurate.

Table I. Thermodynamic Parameters for Lauric Acid Mesophase Formation [see Eq. (12)] in 0.1 *M* KCl at 32°C

Parameter[a]	Value[b]
θ ($x + y$)	25.5 ± 4.0
ρ (x/y)	1.7 ± 0.21
ϵ ($\log(K_{meso})/\theta$)	4.49 ± 0.01
$-\log K_{sp}$	9.1 ± 0.01

[a] Obtained by nonlinear least-squares optimization.
[b] Expressed as mean ± standard deviation.

A Reexamination of the Self-Association of Lauric Acid to Form Low Molecular Weight Aggregates

Although the excellent agreement of the model calculations with the pH–solubility profile in Fig. 2 and in ultrafiltrates (Fig. 3) suggests that self-association of LA to form dimers or other low molecular weight aggregates is not important under the conditions employed, there is also considerable literature evidence suggesting that LA self-associates in aqueous solutions (7–15). Mukerjee (12), for example, examined Goodman's (26) data for the partitioning of fatty acids between heptane and aqueous buffers at pH 7.45 and concluded that the primary aggregate in aqueous solution is the anion–anion dimer ($A_2^=$) and that all other aggregates are negligible. However, Smith and Tanford (10) concluded from similar data not only that HA_2^- is the primary dimer instead of $A_2^=$, but that higher-order aggregates must also form, in agreement with the titration data of Eagland and Franks (15).

In neutral pH regions, the formation of high molecular weight aggregates (mesophase) has been demonstrated. The existence of this species may have confounded the interpretation of the hydrolysis, partitioning, and surface tension data previously described.

The presence of low molecular-weight self-associated species in ultrafiltered samples would cause positive deviations between the concentrations obtained in ultrafiltered samples and the regression line (Fig. 3), with the extent of deviation dependent on the magnitude of the formation constants. In order to assess the sensitivity of solubility data to dimerization, simulations of solubility assuming the presence of dimers were compared to experimental data. By assuming that the primary self-associated species would be either $A_2^=$ or HA_2^- dimers, the theoretical concentrations in ultrafiltered samples may be expressed by Eq. (6).

Two models of LA dimerization cited in the literature were used to simulate solubility data. The model of Mukerjee (12) assumes that the principal LA dimer is $A_2^=$ with a formation constant, $K_d = 650\ M^{-1}$. Eagland and Franks argued that the principal dimer is not $A_2^=$ but HA_2^- (15), and from their reported values at 25 and 50°C, a K_d of 0.14 M^{-1} and a K_{dh} of $2.5 \times 10^4\ M^{-1}$ were estimated at 32°C.

Values for S_o, pK_a, and K_{sp} required in the simulations were taken from computer fits of Figs. 2 and 3. The simulated effects of dimerization on the concentrations of LA in ultrafiltered samples are shown in Fig. 7 along with the experimental results. As pH increases beyond 6.5, the slope of the log(solubility)–pH profile in Mukerjee's model is greater than the slope of the line through the experimental data, arguing against the formation of anion–anion dimers or *n*-mers. Somasundaran (7), who studied surface tension changes with oleic acid concentration, also suggested that self-association of oleic acid anions to form dimers is much less favorable than suggested by Mukerjee. The pH dependence of LA concentration in ultrafiltered samples is also inconsistent with the formation of acid-soap dimers as assumed by Eagland and Franks (15). These findings agree with those of Lucassen (17), who stated that abnormal hydrolysis behavior could be explained by the presence of different solid phases and was not due to self-association in solution. Cistola *et al.* (2) also found no evidence for premicellar association of fatty acids below the solid → liquid crystal transition temperature of the acid-soaps they investigated. The contribution of low molecular weight aggregates to the total LA concentration therefore appears to be negligible in the systems investigated herein.

Thermodynamics of Lauric Acid Mesophase Formation

Mesomorphic structures (e.g., vesicles, hexagonal phases, inverted hexagonal phases, planar bilayers, and micelles) of fatty acids have previously been reported in solutions at temperatures above the melting points of the corresponding hydrated acid-soaps (1,2,18,27). Cistola *et al.* (1) observed that, depending on temperature, lamellar liquid crystals appeared in solution during the titration of fatty acid micellar solutions with HCl. Hargreaves and Deamer witnessed by phase-contrast microscopy the phase transition of crystalline potassium hydrogen dilaurate to large (0.5 μm < radius < 50 μm) liposomes at 34.0°C (18). In this study, turbidity was observed at temperatures below the phase transition temperature for potassium hydrogen dilaurate (34°C). Indeed, turbidity was evident in samples equilibrated at temperatures as low as 28°C, suggesting that mesophase formation is not a simple phase transition.

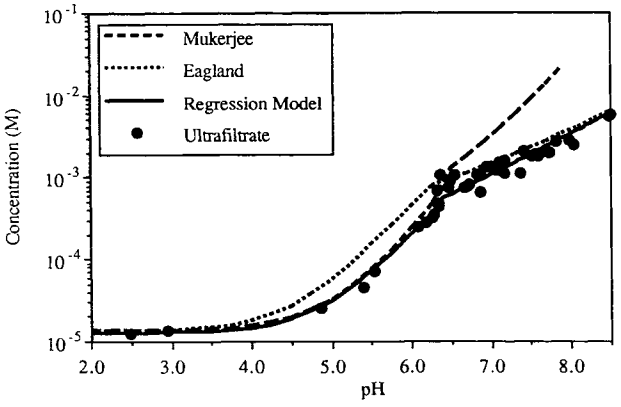

Fig. 7. Comparison of experimental lauric acid concentrations in ultrafiltered samples varying in pH with simulations showing the sensitivity of the lauric acid solubility–pH profile to dimer formation. Mukerjee's model assumes that only $A_2^=$ dimers exist (K_d = 650 M^{-1}), while Eagland and Frank's model assumes the presence of both HA_2^- dimers ($K_{dh} = 2.5 \times 10^4\ M^{-1}$) and $A_2^=$ dimers (K_d = 0.14 M^{-1}).

Mannitol trapping studies (Fig. 6) provide strong evidence that the mesophase consists largely of vesicles as the entrapped volume in filtered samples containing a mesophase was in reasonable agreement with that calculated from the mean hydrodynamic radius of the mesophase particles, assuming that the particles were unilamellar vesicles. Thus, unilamellar vesicles exist in equilibrium with solid phase at temperatures below the phase transition temperature. The ability to measure the LA monomer concentration in the presence of mesophase by ultrafiltration allowed us to develop a mass-action law for mesophase formation. To our knowledge, this is the first such mass-action law describing the thermodynamics of self-assembly of a lipid bilayer.

The relationship developed assumed that the mesophase is a distinct aggregated species with an equilibrium constant, K_{meso}, defined by Eq. (7), containing a fixed ratio of neutral-to-ionized LA. It assumes that the surface charge of the aggregate is completely neutralized by bound potassium ions. The concentration of mesophase, expressed by Eq. (12), is determined by the concentrations of LA monomer, potassium concentration, and pH. Equation (12) contains three adjustable parameters: θ, the index of cooperativity, reflects the total number of molecules of LA and laurate anion within the aggregate; ρ is the free acid:anion ratio within the aggregate; and ϵ is equal to the standard free energy of mesophase formation per monomer divided by $-2.303RT$. As shown by the excellent fit of the model to the experimental data for filtered samples (Fig. 3), this simple mass-action law quantitatively accounts for the peak in mesophase concentration at pH ≈6.5 as well as the peak width and asymmetry.

Computer simulations (not shown) in which each of the parameters were systematically varied indicate that the width of the peak in the mesophase region is a function of θ, the peak symmetry is a function of ρ, and the amplitude depends on ϵ. The very narrow pH range over which mesophase predominates is indicative of the relatively high cooperativity for mesophase formation, as shown by a θ value of ≈25 (Table I). Interestingly, the maximum mesophase concentration occurs at a pH at which both solid LA and potassium hydrogen laurate coexist and declines with further increases in pH. This is a consequence of the nearly twofold excess of free acid in the mesophase (ρ = 1.7), a marked difference from the composition of potassium hydrogen dilaurate, which has an acid:anion ratio of 1. Below pH 6.5 (Fig. 3), the free acid monomer concentration is constant and equal to S_o due to the presence of LA as the solid phase. The mesophase concentration increases with pH as the laurate anion monomer concentration increases within this region. Although the solution concentration of laurate anion continues to increase above pH 6.5, where the solid phase is potassium hydrogen dilaurate, the mesophase concentration decreases due to the higher sensitivity of mesophase formation to the decreasing free acid monomer concentration in solution. From the ρ value obtained from fitting the filtered sample concentrations shown in Fig. 3, the molar fraction of

anion within the mesophase can be estimated to be 0.37, consistent with the value of 0.32 ± 0.04 obtained from the titration analyses of mesophase composition. The constancy in this ratio over the pH range 6.5 to 6.94 further supports the treatment of mesophase formation in terms of a single aggregated species. Evidently, a ratio of free acid to anion >1 is necessary to maintain sufficient spacing between laurate anion head groups within the interfacial region of the bilayer. Additional stabilization may be afforded by hydrogen bonding of $-COOH$ groups at the bilayer surface to adjacent negatively charged $-COO^-$ groups.

The concentration of mesophase in suspensions containing excess LA and potassium hydrogen dilaurate was shown to be highly dependent on KCl concentration, as illustrated in Fig. 5. Due to the common ion effect on the solubility of potassium hydrogen dilaurate, an increase in KCl concentration decreases the laurate anion concentration in solution and therefore the equilibrium pH (experimental equilibrium pH values are shown in parentheses in Fig. 5). Accompanying the decrease in pH is a decline in monomer concentration when both solids are present. This decrease in monomer concentration is amplified by the power θ in the expression for mesophase concentration [Eq. (12)], resulting in a dramatic predicted decline in mesophase concentration with increasing [KCl], which is qualitatively consistent with Fig. 5.

Both QLS measurements and mannitol trapping experiments were consistent with an average particle radius of ≈1000 Å. Assuming that the mesophase particles are unilamellar with a head-group area of 35 Å^2 and a chain length of 15 Å (24), the number of molecules of LA per vesicle was estimated to be $\approx 7 \times 10^5$—several orders of magnitude larger than the aggregate size ($\theta \approx 25$) determined thermodynamically. These results suggest that the mass-action law describing mesophase formation refers to a domain much smaller than the entire vesicle. A suggestion by Lasic (28) regarding the mechanism of phospholipid vesicle formation may have a bearing on these results. He proposed that phospholipid fragments, described as flat disk-shaped micelles, form initially from monomers and then aggregate to form vesicles. Similarly, the mass-action law derived from LA solubility data presented herein implies that a *unit domain* of the mesophase may govern the thermodynamics of vesicle assembly. Israelachvili *et al.* suggested that the minimization of the free energy for lipid bilayer self-assembly involves maintaining critical geometrical packing constraints (29). In addition to an optimal outside-to-inside surface area ratio, there is also likely to be an optimal free acid:anion ratio on both the outer and the inner monolayers. These constraints may require that a minimum free energy is attained only after a specific, critical number of monomers (i.e., a unit domain) have been incorporated into the vesicle.

Related studies with other bilayer forming lipids will be necessary to determine if similar mass-action laws and the concept of a unit domain are generally applicable to the problem of lipid bilayer self-assembly.

ACKNOWLEDGMENTS

This work was supported by a grant from Riker/3M Laboratories. Scott Smith received partial support from a Pharmaceutical Manufacturers Association Advanced Predoctoral Fellowship.

REFERENCES

1. D. P. Cistola, D. Atkinson, J. A. Hamilton, and D. M. Small. Phase behavior and bilayer properties of fatty acids: Hydrated 1:1 acid-soaps. *Biochemistry* 25:2804–2812 (1986).
2. D. P. Cistola, J. A. Hamilton, D. Jackson, and D. M. Small. Ionization and phase behavior of fatty acids in water: Applications of the Gibbs phase rule. *Biochemistry* 27:1881–1888 (1988).
3. J. E. Staggers, O. Hernell, R. J. Stafford, and M. C. Carey. Physical-chemical behavior of dietary and biliary lipids during intestinal digestion and absorption. I. Phase behavior and aggregation states of model lipid systems patterned after aqueous duodenal contents of healthy adult human beings. *Biochemistry* 29:2028–2040 (1990).
4. B. J. Aungst. Structure/effect studies of fatty acid isomers as skin penetration enhancers and skin irritants. *Pharm. Res.* 6:244–247 (1989).
5. S. Muranishi. Absorption barriers and absorption promoters in the intestine. In D. D. Breimer and P. Speiser (ed.), *Topics in Pharmaceutical Sciences*, Elsevier/North-Holland, Amsterdam, 1987, p. 445.
6. T. Sawada, T. Ogawa, M. Tomita, M. Hayashi, and S. Awazu. Role of paracellular pathway in nonelectrolyte permeation across rat colon epithelium enhanced by sodium caprate and sodium caprylate. *Pharm. Res.* 8:1365–1371 (1991).
7. P. Somasundaran, K. P. Ananthapadmanabhan, and I. B. Ivanov. Dimerization of oleate in aqueous solutions. *J. Coll. Interface Sci.* 99:128–135 (1984).
8. G. Stainsby and A. E. Alexander. Studies of soap solutions. *Trans. Faraday Soc.* 45:585–597 (1949).
9. I. Danielsson and P. Stenius. Anion association and micelle formation in solutions of hydrotropic and short-chain carboxylates. *J. Coll. Interface Sci.* 37:264–280 (1971).
10. R. Smith and C. Tanford. Hydrophobicity of long chain n-alkyl carboxylic acids, as measured by their distribution between heptane and aqueous solutions. *Proc. Natl. Acad. Sci. USA* 70:289–293 (1973).
11. J. Powney and D. O. Jordan. The hydrolysis of soaps as determined from glass electrode pH measurements. *Trans. Faraday Soc.* 34:363–371 (1938).
12. P. Mukerjee. Dimerization of anions of long-chain fatty acids in aqueous solutions and the hydrophobic properties of the acids. *J. Phys. Chem.* 69:2821–2827 (1965).
13. K. P. Ananthapadmanabhan and P. Somasundaran. Acid-soap formation in aqueous oleate solutions. *J. Coll. Interface Sci.* 122:104–109 (1988).
14. M. A. Cook. Mechanism of hydrolysis in aqueous soap solutions. *J. Phys. Chem.* 55:383–402 (1951).
15. D. Eagland and F. Franks. Association equilibria in dilute aqueous solutions of carboxylic acid soaps. *Trans. Faraday Soc.* 61:2468–2477 (1965).
16. M. E. Feinstein and H. Rosano. The influence of micelles on titrations of aqueous sodium and potassium soap solutions. *J. Phys. Chem.* 73:601–607 (1969).
17. J. Lucassen. Hydrolysis and precipitates in carboxylate soap solutions. *J. Phys. Chem.* 70:1824–1830 (1966).
18. W. R. Hargreaves and D. W. Deamer. Liposomes from ionic, single-chain amphiphiles. *Biochemistry* 17:3759–3768 (1978).
19. R. A. Robinson and R. H. Stokes. *Electrolytic Solutions*, Butterworths, London, 1959.
20. J. O. Bockris and A. K. Reddy. *Modern Electrochemistry*, Plenum, New York, 1973.
21. E. D. Goddard, S. Goldwasser, G. Golikeri, and H. C. Kung. Molecular association in fatty acid-potassium soap systems. *Adv. Chem. Ser.* 84:67–77 (1968).
22. G. H. Bell. Solubilities of normal aliphatic acis, alcohols and alkanes in water. *Chem. Phys. Lipids* 10:1–10 (1973).
23. P. Schurtenberger, N. Mazer, and W. Kanzig. Micelle to vesicle transition in aqueous solutions of bile salt and lecithin. *J. Phys. Chem.* 89:1042–1049 (1985).

24. J. N. Israelachvili, D. J. Mitchell, and B. W. Ninham. Theory of self-assembly of lipid bilayers and vesicles. *Biochim. Biophys. Acta* **470**:185–201 (1977).
25. A. N. Campbell, N. O. Smith, and A. Findlay. *The Phase Rule and Its Applications,* Dover, New York, 1951.
26. D. S. Goodman. The distribution of fatty acids between n-heptane and aqueous phosphate buffer. *J. Am. Chem. Soc.* **80**:3887–3892 (1958).
27. P. Ekwall. Composition, properties, and structures of liquid crystalline phases in systems of amphiphilic compounds. In G. H. Brown (ed.), *Advances in Liquid Crystals,* Academic Press, New York, 1975, pp. 1–145.
28. D. Lasic. The mechanism of vesicle formation. *Biochem. J.* **256**:1–11 (1988).
29. J. N. Israelachvili, S. Marcelja, and R. G. Horn. Physical principles of membrane organization. *Q. Rev. Biophys.* **13**:121–200 (1980).